JOURNAL OF GEOPHYSICAL RESEARCH, VOL. 90, NO. C3, PAGES 5035-5044, MAY 20, 1985

ACTIVE MICROWAVE MEASUREMENTS OF ARCTIC SEA ICE UNDER SUMMER CONDITIONS

R. G. Onstott and S. P. Gogineni

Remote Sensing Laboratory, University of Kansas Center for Research, Inc., Lawrence

Abstract. Helicopter-borne L-C-X-Ku-band radar backscatter data were acquired over test sites in the region about Saint Patrick Island, Northwest Territory, Canada, during June 1982. It is shown that the microwave response of sea ice is greatly influenced by summer, due to the many changes in properties of the snowpack and ice sheet. Hence the well-documented winter-and-spring microwave response may not be extended into the summer season. In summer, the scattering cross sections of multiyear and first-year ice become very similar, and their contrast is not only greatly reduced, but exhibits reversals in strength. During the early part of summer, discrimination was similar at all frequencies between 4 and 18 GHz with first-year ice returns slightly stronger than those of multiyear ice. However, during peak melt, when the first-year ice was extensively flooded and produced weaker returns than multiyear ice, operation at lower frequencies, especially L-band, showed a 2-3 dB discrimination advantage. Angles greater than 25° from vertical provided the best contrast.

Introduction

The value of all-weather, day-night reconnaissance radar has been well established. Radar is recognized as a significant tool in the study of sea-ice science and in sea-ice operational problems [Rouse, 1969; Johnson and Farmer, 1971; Parashar et al., 1974; Gray et al., 1977; Campbell, 1978; Livingstone et al., 1980; Ketchum and Tooma, 1973; Larson et al., 1981; Weeks, 1981; Luther et al., 1982]. This is particularly impressive in that these radars have not been optimized for ice studies.

Many physical parameters that are important to the science of sea ice may be measurable using radar as an operational tool. Given a radar remote sensing system whose frequency of operation, range of viewing angles, selection of antenna polarizations, and resolution have been optimized, a whole host of scene parameters may be extractable from space or aircraft. These may include the fraction of a region that is covered by ice, the distribution of thickness categories, floe sizes, ridge and rubble distribution patterns, leads, ice islands, ice motion, icebergs, ice surface roughness, ice properties, and the study of the seasonal advance and retreat of the seaward edge of the regional pack ice.

Because the observational capability of radars in space and in aircraft has been so clearly proven as to their research and operational potential, the United States and Canada have undertaken studies to define a bilateral synthetic aperture radar (SAR) satellite program [Raney, 1982; Weeks and Untersteiner, 1980]. These studies, the Free-Flying Imaging Radar Experiment in the United States and the Radar Satellite Project in Canada, address the requirements for such a SAR mission: science and operations in sea-ice-covered waters, oceanography, renewable resources, and nonrenewable resources. The work addressed in this paper concerns the needs associated with the study of sea-ice-covered waters. Before a research or operational spaceborne SAR or real aperture radar (RAR) can be built for effective use, an adequate knowledge of the backscatter coefficients of ice features of interest is necessary.

Radar returns from the planetary surface are described by a scattering coefficient (backscattering cross section per unit area). Since the total cross section of a pixel varies with the illuminated area, and this is determined by the radar geometric parameters (pulsewidth, beamwidth, etc.), the scattering coefficient was introduced to obtain a coefficient independent of these parameters.

Two major classes of parameters which influence radar earth returns are the radar system parameters and the earth scene parameters. To describe the influence of the radar parameters, backscatter measurements are made as a function of radar frequency, viewing angle, and antenna polarization. The earth scene parameters, examined directly or indirectly through characterization measurements, include (1) complex permittivity, (2) roughness of surface and substances to depths where attenuation reduces the electromagnetic wave to negligible amplitude, and (3) location and size of scattering centers. Because the physical and electrical properties of ice are influenced by season, it is necessary to have a season-dependent description of the backscatter properties.

Backscatter coefficients are useful in many ways. Not only do they allow the specification of new remote sensors, but they also are useful in the interpretation of data products from existing and future sensors. Comprehensive backscatter measurement and ice characterization programs enhance our ability to understand and study the radar-ice interaction process.

The University of Kansas spectrometer/scatterometer measurements have been made over a wide range of frequencies (L-C-X-Ku bands). In contrast, in the past, investigations have been limited to one or two frequencies. Previous investigations at L-, X-, and Ku-band frequencies during the winter and spring have shown that frequencies above 9 GHz have the ability to discriminate between different ice types, while frequencies below 1.5 GHz do not [Onstott and Kim, 1983; Onstott et al., 1982a]. A recent investigation during the fall of 1981 [Gray et al., 1982;

Paper number 4C1283.
0148-0227/85/004C-1283$05.00

Fig. 1. University of Kansas helicopter-borne side-looking spectrometer/scatterometer.

Onstott et al., 1982b] has shown that there is a greater similarity in the ability to discriminate ice-types between C-band and X- and Ku-band frequencies than between C-band and L-band frequencies. Even though contrast at C-band frequencies was reduced, there was still a very good ability to discriminate in the fall.

The purpose of this investigation is to study the influence of summer upon the discrimination capability at all frequencies (1-18 GHz) so that it is known whether an active remote sensor is useful in all seasons or whether seasonal effects can cause ambiguities. It had been suggested, prior to this investigation, that the longer wavelengths, such as C-band, may be less influenced by the effects of the melt season. Even though the ability to discriminate at even the higher frequencies has not been adequately described, this suggested the potential all-season utility of a longer wavelength sensor.

A majority of all the remote sensing experiments have taken place during winter or spring. Few have taken place in the summer, and only in the most recent investigations has there been coordination of an extensive surface observation program which detailed the state of the snow-covered ice sheet, surface-based active and passive measurements, and airborne active and passive measurements. Previously available information concerning the ability of radar to discriminate ice types in the summer has been limited to the observations made by Onstott et al. [1982b] in the Greenland Sea in August of 1980, by Gray et al. [1982] in the Beaufort Sea in June/July of 1980, and by Peteherych [1981] using data acquired from the SEASAT scatterometer. Results of the August investigation and the SEASAT data set show a reversal of cold weather trends with first-year ice having cross sections that are higher in absolute level than those of multiyear ice and that the multiyear ice had levels which were greatly reduced from winter levels. The Beaufort Sea data set for sea ice under its peak melt condition (measurements made around the first of July) showed multiyear scattering cross sections which departed from its typical winter trend and had become nearly identical to those of first-year ice, which were not significantly different from its winter cross sections even though significant changes were noted in the state of the ice and snow.

Description of Experiment

An investigation of first-year and multiyear ice during the summer melt season was made in June 1982 at Mould Bay, Northwest Territories, Canada (76°14'N, 119°20'W). This program was many faceted and included coincident active near-surface measurements (this paper) and passive near-surface measurements [Grenfell and Lohanick, this issue], intensive ice characterization [Holt

TABLE 1. Nominal System Specifications

	C-X-Ku Band	L-Band
Type	FM-CW	FM-CW
Frequency range	4-18 GHz	1-2 GHz
Modulation	Triangular	Triangular
Sweep bandwidth	750 MHz	800 MHz
Transmitter power	10-19 dBm	19 dBm
IF frequency	50 kHz	50 kHz
IF bandwidth	13.5 kHz	13.5 kHz
Antennas	Parabolic reflectors with log-periodic feeds	
Polarization	VV	
Size	46 cm	
Beamwidths	6.4°, 4.4°, 3.8° and 3.4° at 4.8, 7.2, 9.6 and 13.6 GHz	
Polarization	HH	HH
Size	61 cm	46 and 61 cm
Beamwidths	5.0°, 3.4°, 2.5° and 1.9° 4.8, 7.2, 9.6 and 13.6 GHz	11.4°
Polarization	HV	
Size	46 cm and 61 cm	
Beamwidths	5.6°, 3.8°, 3.4° and 2.6° at 4.8, 7.2, 9.6 and 13.6 GHz	
Incidence angles	5° - 70°	5° - 70°
Calibration		
Relative	Delay line	Delay line
Absolute	Luneberg lens	Corner reflector
Altitude	30 m for θ = 5 to 21 15 m for θ > 30	30 m for θ = 5 to 21 15 m for θ > 30

and Digby, this issue], ice microstructure work, lead dynamics, and active and passive aircraft overflights (Atmospheric Environment Service side-looking airborne X-band radar and Canadian Center for Remote Sensing synthetic aperture X-band radar, Ku-band radiometer, and Ku-band scatterometer [Livingstone, this issue]). Also, to aid in the investigation of the radar-ice interaction properties, detailed ice surface roughness measurements were made.

Sensor Description

The sensor used in the near-surface radar experiments was a wideband frequency-modulated continuous-wave radar spectrometer which operated over the frequency range from 1 to 18 GHz, angles from 5° to 60°, and at like- and cross-antenna polarizations. The side-looking radar spectrometer was operated from a Bell Model 206 helicopter (see Figure 1). Nominal system specifications are detailed in Table 1.

Relative calibration of the system was acquired by frequently measuring the signal from a delay line switched in place of the antenna. Absolute calibration was established by measuring the received power from targets of known radar scattering cross sections (Luneberg lens and trihedral corner reflector).

The statistical properties of the received signal from a distributed target are typically Rayleigh-like. Many independent samples have been averaged, reducing the effects due to fading [Ulaby et al., 1982], thereby providing an accurate estimate of the mean cross section. Independent samples were obtained by sweeping with a bandwidth in excess of that required for resolution and by spatial sampling. Table 2 has been presented to provide the order of magnitude of the number of independent samples obtained in these measurements. Some 250, 500, and 1000 independent samples are necessary to reduce the 90% confidence interval to ±0.4, ±0.3, and ±0.2 dB, respectively.

TABLE 2. Typical Minimum Number of Independent Samples Acquired During Measurements

	Spatial Samples Frequency (GHz)				Frequency Averaged Samples Frequency (GHz)				Detector Averaged Samples Frequency (GHz)				Total Independent Samples Frequency (GHz)			
Angle	1.5	5.2	9.6	13.6	1.5	5.2	9.6	13.6	1.5	5.2	9.6	13.6	1.5	5.2	9.6	13.6
0	25	25	25	25	4	1	1	1	10	10	10	10	1,000	250	250	250
20	25	25	25	25	8	3	1	1	10	10	10	10	2,000	750	250	250
30	25	100	100	100	14	5	2	2	10	10	10	10	3,500	5,000	2,000	2,000
40	35	100	100	100	24	7	4	3	10	10	10	10	8,400	7,000	4,000	3,000
50	50	100	100	100	34	13	7	5	10	10	10	10	17,000	13,000	7,000	5,000
60	100	100	100	100	45	24	12	9	10	10	10	10	45,000	24,000	12,000	9,000

TABLE 3. Summary of Sites Investigations and Comments About Ice Conditions

Site	Type	Date	Depth, m Ice	Depth, m Snow	Temperature, °C Air	Temperature, °C Ice	Avg. Salinity, m Top 0.10,	Avg. Salinity, m Top 0.50,	Comments
Mould Bay	FY	June 21	2.25	0.02-0.01	2.2	0.1	1.54	2.84	Ice surface was rough and had a wet snow cover.
		June 29	2.11	0.00	2.0	0.0	2.88	3.72	90% of surface area covered with water.
Peach Pit	FY	June 22	1.88	0.02-0.05	2.5	0.0	1.16	3.06	Ice surface had varying degrees of surface roughness.
		July 2	1.83	0.0	4.0	0.0	2.30	3.11	Large portion of ice was flooded.
	MY	June 22	>3.0	0.01-0.02	2.5	0.0	0.05	0.19	Hummocks were wet with significant small-scale roughness.
Intrepid	MY	June 26	>4.0	0.01-0.03	3.0	0.0	0.21	0.70	Hummocks were wet and smooth.
Pay Day	MY	June 30	>4.0	0.01-0.02	4.2	0.0	0.17	0.18	Ice was saturated with water.
	FY	July 3	1.00	0.00	4.0	0.0	2.10	2.80	Over 80% of surface was covered with water.

Description of Sites

Four experiment sites in the waters around Mould Bay were investigated: (1) first-year ice in Mould Bay, (2) a composite floe of multiyear ice frozen in first-year ice (Peach Pit), (3) an old multiyear floe frozen in first-year ice (Intrepid), and (4) a composite of first-year ice and multiyear ice in the Beaufort Gyre (Pay Day). Characterization measurements were made to provide detailed descriptions of the site under investigation at the time of the backscatter measurement [Holt and Digby, this issue; Onstott and Gogineni, 1983]. Description of the snowpack included depth; density; snow surface temperature; a general description of grain size, shape, and texture; and snowpack structure. Description of the ice sheet included type, thickness, surface roughness, surface temperature, salinity profile, and surface water. A summary of the sites and general characteristics are given in Table 3.

The first-year ice had begun the season with a thickness of approximately 2 m and had salinities

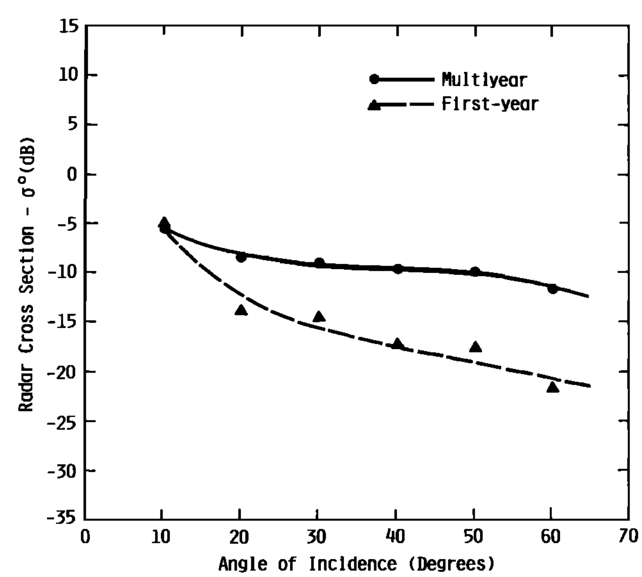

Fig. 2. Scattering coefficients of multiyear and first-year sea ice under cold late fall conditions at 9.6 GHz and HH-polarization (October 1981).

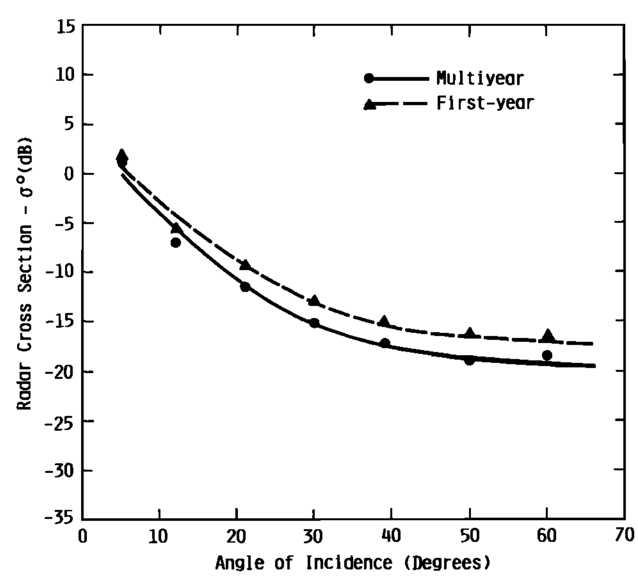

Fig. 3. Scattering coefficients of multiyear and first-year ice under summer melt conditions at 9.6 GHz and HH-polarization (June 19 and 22, 1982).

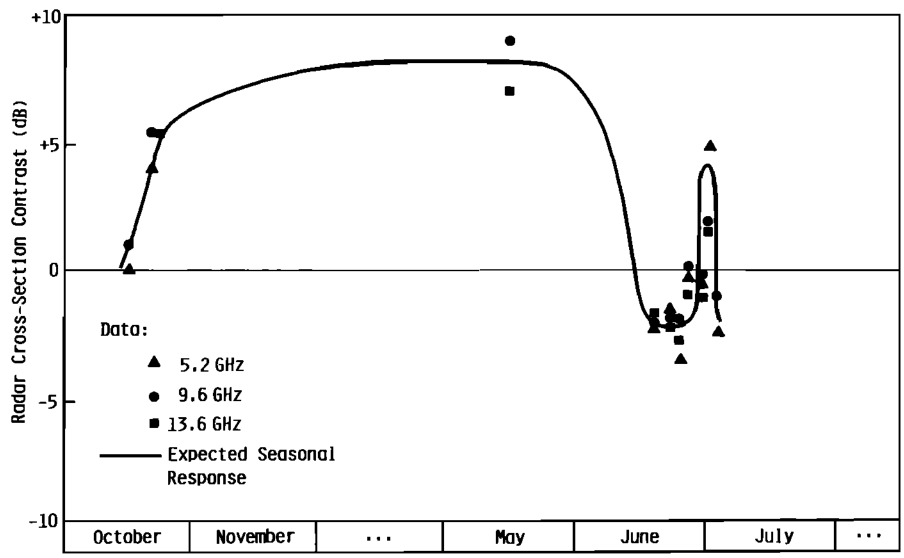

Fig. 4. Expected and measured radar cross-section contrast history for multiyear and first-year ice at 5.2, 9.6, and 13.6 GHz with HH-polarization and an angle of 30°.

of 1-3 ppt in the top 10 cm and 3-4 ppt in the top 50 cm. Multiyear ice had a thickness that was much greater than 3 m and salinities of 0-0.5 ppt in the top 10 cm and 0.2-0.7 ppt in the top 50 cm. The snowpack and ice sheet experienced many distinct transitions in their properties due to the influence of summer. Changes in experiment sites were dramatic and detectable on at least a daily basis.

Results

Active microwave observations of Arctic sea ice are most interesting and complex in the summer due to an almost constant change in physical and electrical properties. At summer's onset, when this investigation began, snowpack was in place in a fashion very similar to that found in winter and spring. As ambient air temperatures climbed, free water became present in the now humid snowpack and, influenced by a cold ice-snow interface, ice crystals enlarged by restructuring. As melt intensified, water percolated through the snow and, in particular on first-year ice, collected and froze on the ice surface, creating a superimposed ice layer [Jacobs et al., 1975]. The initial addition of ice occurred over the span of, at most, 3 days (observations were documented during surface roughness measurements) and resulted in a dramatic increase in surface roughness over once basically smooth, first-year ice. During the next prominent transition, the major part of the snowpack had melted away, creating standing water. Mounds of restructured snow and ice of snowdrift origin provided the only interruption in the scene's topography. Multiyear ice was also composed of two distinct features: ice mounds covered by a crust of millimeter diameter ice crystals and meltpools. During mid-summer peak melt, multiyear meltpools became extensive, and first-year ice exhibited up to 90% area coverage of standing water. First-year ice then showed cycles of draining and melting. By summer's end, it was observed that first-year ice drained and remained drained.

It has been well documented that, during winter, spring, and late fall, there is a significant separation between the scattering cross sections of the two major summer ice types and that there is a remarkable ability to discriminate with radars operating with the appropriate parameters. However, during summer this contrast was greatly reduced. Throughout the early part of summer there was a reordering of scattering cross sections with first-year ice returns greater than those of multiyear ice for frequencies in the range from 4 to 18 GHz. L-band measurements were not made until mid summer. Figures 2 and 3 graphically show the angular response of the radar cross sections of multiyear and first-year ice during both early summer and

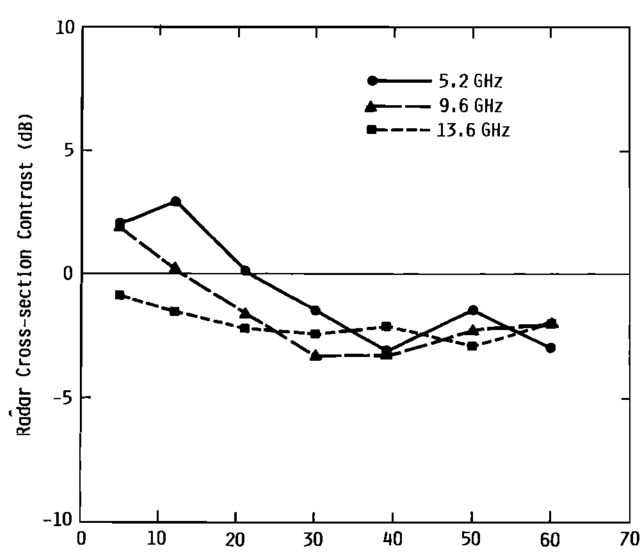

Fig. 5. Radar cross-section contrast between multiyear and first-year ice at 5.2, 9.6, and 13.6 GHz with HH-polarization for early summer melt conditions (June 19 and 22, 1982).

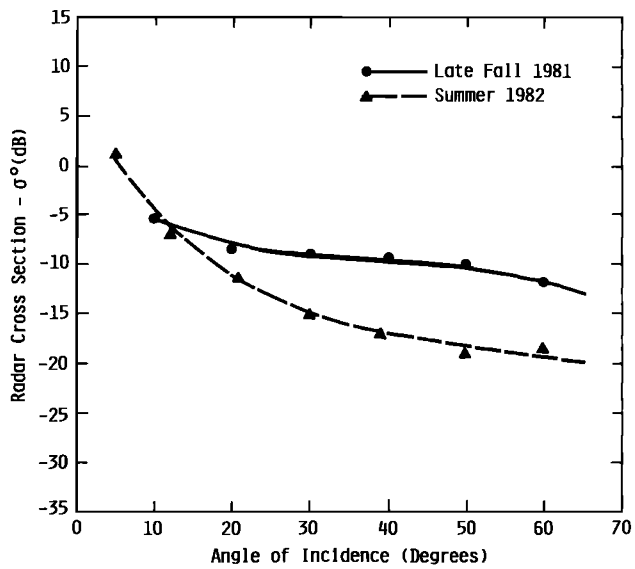

Fig. 6. Scattering coefficients of multiyear ice under cold late fall and early summer melt conditions at 9.6 GHz and HH-polarization (October 1981 and June 19 and 22, 1982).

the cold conditions of late fall. The ability to discriminate between these ice types, based upon the strength of return, is still possible. Even as summer progressed, with the snowpack disappearing and the ice becoming very wet, results show that a discrimination capability did exist; however, a priori knowledge is probably needed, and discrimination analyses will be based upon the distribution of the ice and water features which are correlatable with ice type. Multiyear ice did not loose its ice-surface area at the same rate as first-year ice and therefore had less area covered with water. There may be times (possibly around June 15 and July 1) in which the snowpack or the surface of both ice types may be so wet that there will be only a marginal ability to discriminate. This may, however, only be a problem during portions of a day due to refreezing during summer's night and may exist over a period of a few days. The seasonal change in contrast between these two important ice types is shown in Figure 4. This illustrates the significant influence summer melt has on the backscatter process. Results show that contrast information was similar at frequencies from 4 to 18 GHz for angles greater than 20° (see Figure 5).

The departure of summer from winter trends for multiyear ice is most dramatic. Cross sections are reduced by many decibels (8 dB at 9.6 GHz, HH-polarization and 40°) and retain levels at or below those of winter, spring, or fall first-year ice (see Figure 6). This decrease is explained by examining the influence of summer melt on two mechanisms which control the backscatter process. Under cold conditions, when the radar signal penetrates the slightly lossy multiyear ice sheet whose large bubbles in its upper layer act as scattering centers, volume scattering plays an important role in producing its characteristically high backscatter levels which decay slowly with increasing angle. In the summer, free water on the ice surface, in the ice, and in the snowpack inhibit the ability of the radar signal to penetrate to a degree necessary for a significant volume-scattering contribution; thus the backscattering process is dominated by surface scattering from the ice sheet and/or absorption by the snowpack, since surface scattering from undisturbed snowpack is weak. This is similar to the scattering process of first-year ice, in which there is little ability of the radar signal to penetrate the ice sheet during winter due to the large losses attributable to high brine concentrations and during summer when free water content limits scattering to surface effects.

The seasonal response of first-year ice is also interesting because there is an increase in scattering cross sections from winter to summer (see Figure 7). This increase becomes expected due to the observed dramatic increase in surface roughness created by the combined effect of the addition of a superimposed ice layer, the recrystallization action which transforms the snowpack into a dense material, and an increased reflection coefficient attributed by melt and/or a temperature-induced increased dielectric constant. Figure 8 shows a histogram of two roughness conditions for homogeneous first-year ice measured 5 days apart. The roughness illustrated in Figure 8a (June 14) is representative of smooth ice under fall, winter, spring, and premelt conditions. The roughness shown in Figure 8b (June 20) is representative of smooth ice which has experienced the addition of melt-induced superimposed ice. As is clearly seen, the addition of such an ice layer dramatically increases small-scale surface roughness to which the higher frequency microwave radars are extremely sensitive. The range between maximum and minimum roughness features increased by a factor of 3 when the superimposed ice was added. If it were not for the high two-way path losses associated with the remaining wet snow layer, there would have been an even more

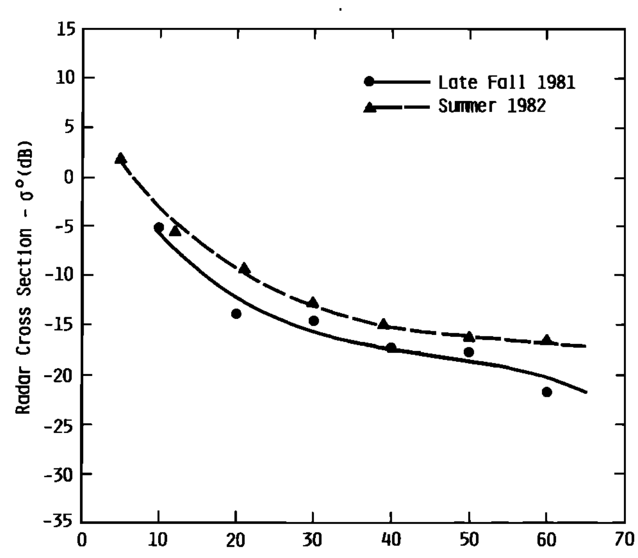

Fig. 7. Scattering coefficients of first-year ice under cold late fall and early summer melt conditions at 9.6 GHz and HH-polarization (October 1981 and June 19 and 22, 1982).

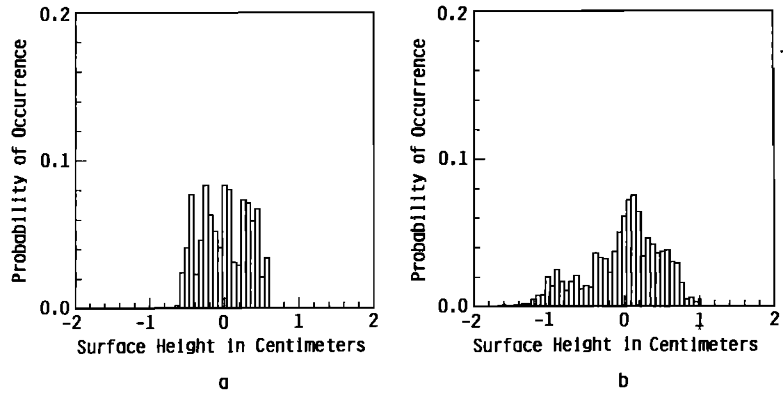

Fig. 8. First-year ice surface height histograms for a homogeneous ice sheet. (a) Data acquired June 14 are typical of early summer pre-melt, late fall, winter, and spring conditions. Height range, variance, and skewness were 0.932 cm, 0.044 cm^2, and 0.0003, respectively. (b) Data acquired June 20 are typical of early summer melt conditions. Superimposed ice increased the height range to 2.778, the variance to 0.243, and skewness to -0.588.

dramatic increase (our theoretical modeling suggested an increase in the range of 8-10 dB) in the backscatter level of first-year ice than the 2-3 dB observed. When the response of the 8 km Mould Bay profile of homogeneous first-year ice is compared with that obtained in a previous fall experiment (Figure 9), the sensitivity of the radar to small-scale surface roughness is illustrated. The uniformity in the early summer microwave response suggests that the surface has become more uniformly rough in the small scale except for a band of previously rough ice located at the beginning of the line, and that the summer ice sheet has experienced a phenomenon which has superimposed ice very uniformly over the entire sheet and not just in localized areas.

A subtle, but important, observation was that the dynamics of the absolute backscatter level was more of a function of the state of the ice, snow, and standing water than of ice type. This greatly impacts the application of automatic classification schemes for summer ice-type discrimination. Returns for these ice types were slightly separated in absolute level much of the time and each tracked the change in the state of their physical properties. As an illustration, Figure 10 shows the effect of melt on the angular response on the radar cross section of first-year ice at 5.2 GHz and HH-polarization. At the beginning of summer (June 19 and 22), the response was similar to that for late fall conditions. Its cross section, then, increased due to an increase in surface roughness because of the influence of superimposed ice and the erosion and restructuring of its snowpack (June 24). By the middle of the season (July 1), when melting was at its peak, ice mounds (remnants of snow drifts) became extremely wet and smooth, and were the only breaks in the scene composed of great expanses of standing water. Thus first-year ice evolved into a specular-like radar scene. Scattering cross sections exhibited a rapidly decaying response at large angles and an enhanced response near vertical. During this period, multiyear cross sections became greater than those of first-year ice, a significant reversal in ordering from early summer trends. This contrast (Figure 11) was also found to

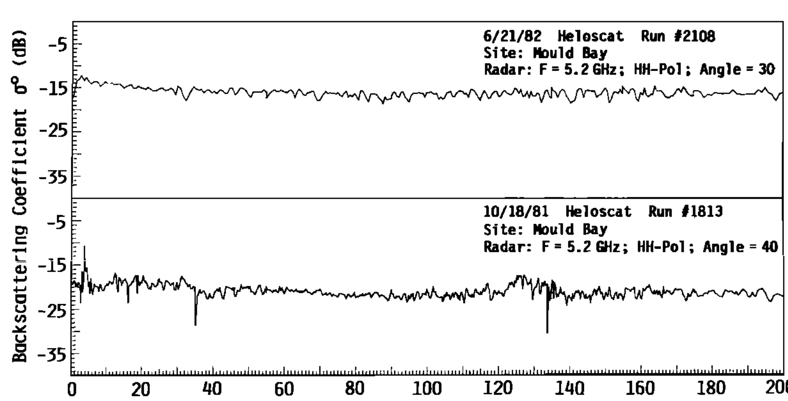

Fig. 9. Scattering cross-section profile of an 8-km line across the homogeneous first-year ice in Mould Bay acquired under late fall and early summer conditions at 5.2 GHz, HH-polarization, 30° and 40°.

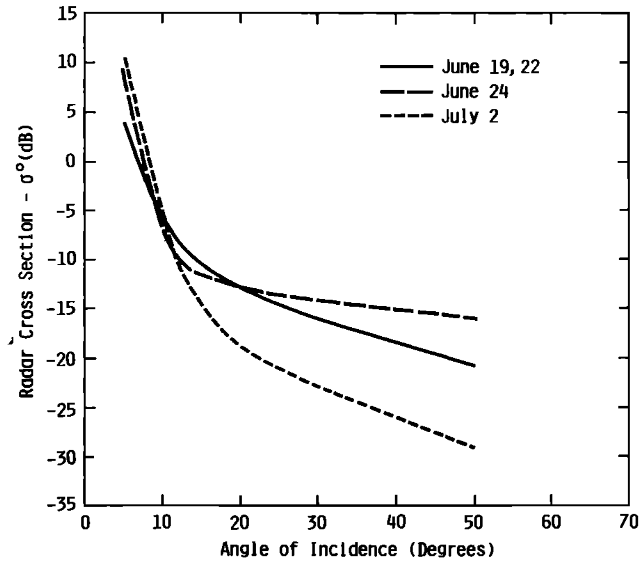

Fig. 10. Scattering coefficients of first-year ice during premelt, melt, and peak-melt conditions at 5.2 GHz and HH-polarization.

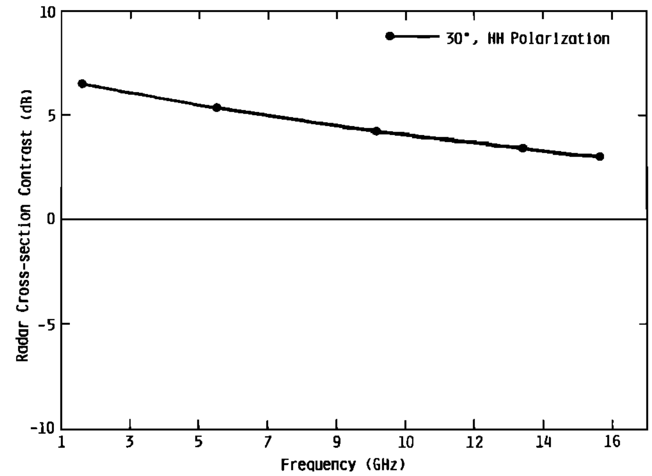

Fig. 11. Radar cross-section contrast between multiyear and first-year ice as a function of frequency for peak melt conditions (July 2).

increase with decreasing frequency and was the greatest at 1.5 GHz. Therefore first-year ice is becoming more smooth looking due to the increase in radar wavelength, while multiyear ice maintains its scene identity. The large, well-defined mounds of ice, with up to 1-m heights, on the multiyear ice serve as the borders of meltpools or meltpool networks and constrain the location of surface water. Hence the areal extent of open water was much less than that observed on the flooded first-year ice. The distribution of these two prominent and important features accounts for the ability to discriminate under peak melt conditions because water in meltpools typically produces much lower returns than ice features. Scatterometer tracks across Intrepid Inlet floe (Figure 12) acquired at 1.5 GHz, HH-polarization, and 12° and 30° show very weak returns for flooded first-year ice, while multiyear ice returns show large variations due to the dissimilarity in its scene constituents. Similar results were observed in imagery obtained at X-band by the AES Electra on July 7.

Conclusions

Helicopter-borne L-C-X-Ku-band calibrated radar data were acquired over areas of Arctic first-year and multiyear ice during the first half of the summer of 1982 at Mould Bay, Northwest Territories, Canada. Results show that the microwave response of sea ice is greatly influenced by summer melt, which causes many changes in the properties of the snowpack and ice sheet. The well-documented winter-and-spring microwave response for cold conditions may not be extended into the summer season.

Backscatter in summer is affected by scattering from wet ice surfaces, an increase in the surface roughness of first-year ice due to the addition of a melt-induced superimposed ice layer, by the absorption of the radar energy by layers of wet snowpack, by the recrystallization action which transforms the snowpack into a dense material, and/or by water standing on a flat ice sheet or enclosed in well-defined pools. The ability to discriminate the two major summer ice types (especially with automatic classification schemes) is complicated because each provides similar backscatter intensities whose absolute

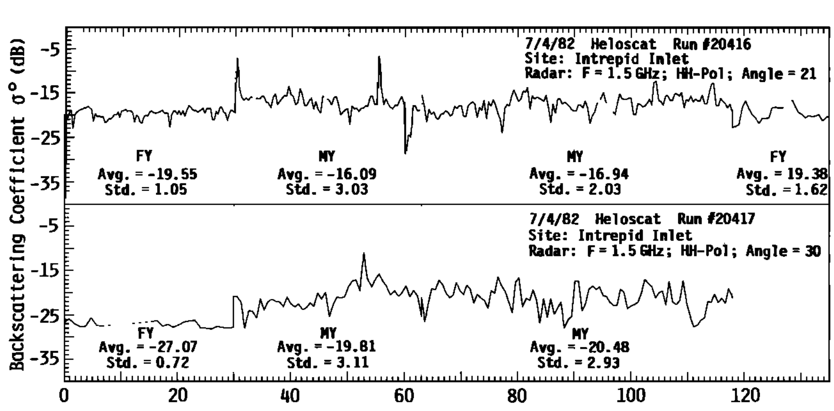

Fig. 12. Scattering cross-section profile across an old multiyear floe frozen in first-year ice in Intrepid Inlet. The radar parameters are 1.5 GHz, HH-polarization, 21° and 30° (July 4).

levels change with the state of the ice sheet and snowpack and each exhibit reversals in their absolute levels which arise because of the many transformations in the scene's physical and electrical properties. During the early part of summer, operation at frequencies from 4 to 18 GHz provided similar discrimination capability while, under peak melt conditions, operation at the lowest frequencies in the range from 1 to 18 GHz provided significantly greater contrast.

We believe that discrimination is possible in the summer by using intensity, shape, and texture in the analysis of data acquired from a multiparameter sensor whose choice of parameters has been optimized. This becomes an especially reasonable expectation if frequent scene coverage is provided. We also believe that there will be good ability to detail the state of the snowpack and the ice sheet.

Since this investigation did not extend beyond the peak melt of summer, it is only conjecture that once the two ice types arrive at a point at which they no longer exhibit large areas of open water they will both provide a scene composed of varying degrees of surface erosion. Identification of large-scale features found on many multiyear floes may allow some measure of discrimination capability as the first-year ice graduates into second-year ice, which does not happen, officially, until October.

Acknowledgments. We would like to express our thanks to R. O. Ramseier, W. F. Weeks, and F. D. Carsey for their efforts toward development and support of the RADARSAT/FIREX program and subsequent investigations. The support by NASA Headquarters (grant NAGW-334) and the Office of Naval Research (contract N00014-76-C-1105), Canadian AES, Canadian NRC, and Canadian PCSP was invaluable. On-site support by Larry Solar, Ken Asmus, David Short, and Susan Digby was much appreciated.

References

Campbell, W. J., J. Wayenberg, J. B. Ramseyer, R. O. Ramseier, M. R. Vant, A. Redmond, L. Arsenault, P. Gloersen, H. J. Zwally, T. T. Wilheit, T. C. Chang, D. Hall, L. Gray, D. C. Meeks, M. L. Bryan, F. T. Barath, C. Elachi, F. Leberl, and T. F. Farr, Microwave remote sensing of sea ice in the Aidjex main experiment, Boundary Layer Meteorol., 3, 309-337, 1978.

Gray, A. L., R. K. Hawkins, C. E. Livingstone, L. D. Arsenault, and W. M. Johnstone, Simultaneous scatterometer and radiometer measurements of sea-ice micro- wave signatures, IEEE J. Oceanic Eng., OE-7(1), 20-32, 1982.

Gray, A. L., R. O. Ramseier, and W. J. Campbell, Scatterometer and SLAR results obtained over Arctic Sea ice and their relevance to the problems of arctic ice reconnaissance, Proceedings of the 4th Canadian Symposium on Remote Sensing, pp. 424-443, Quebec, Canada, May 1977.

Jacobs, J. D., R. G. Barry, and R. L. Weaver, Fast ice characteristics, with special reference to eastern Canadian Arctic, Polar Rec., 17(110), 521-536, 1975.

Johnson, J. D., and L. D. Farmer, Use of side-looking airborne radar for sea ice identification, J. Geophys. Res., 76(9), 2138-2155, 1971.

Ketchum, R. D., and S. G. Tooma, Analysis and interpretation of airborne multifrequency side-looking radar sea ice imagery, J. Geophys. Res., 78(3), 520-538, 1973.

Larson, R. W., J. D. Lyden, R. A. Shuchman, and R. I. Lowry, Determination of backscatter characteristics of sea ice using synthetic aperture radar data, Rep. 142600-1-F, Environ. Res. Inst. of Mich., Ann Arbor, March 1981.

Livingstone, C. E., R. K. Hawkins, A. L. Gray, L. D. Arsenault, K. Okamoto, T. L. Wilkinson, and D. Pearson, The CCRS/SURSAT Active-Passive Experiment 1978-1980. The microwave signatures of sea-ice types and features and their implications for remote sensing, Canada Centre for Remote Sensing, Ottawa, Ont., Canada, June 1983.

Luther, C., J. D. Lyden, R. Shuchman, R. W. Larson, Q. A. Holmes, D. R. Nuesh, and R. T. Lowry, Synthetic aperture radar studies of sea ice, Proceedings of IGARSS, vol. 2, pp. 1.1-1.9, IEEE, New York, 1982.

Onstott, R. G., and S. Gogineni, Characterization measurements of sea ice under summer conditions at Mould Bay during June 1982, Tech. Memo. 331-31/578-3, pp. 1-17, Remote Sensing Lab., Univ. of Kans. Center for Res., Inc., Lawrence, Sept. 1983.

Onstott, R. G., and Y. S. Kim, Preliminary report on active microwave measurements of sea ice under fall conditions--the RADARSAT/FIREX fall experiment, Tech. Rep. 331-31/578-3, Remote Sensing Lab., Univ. of Kans. Center for Res., Inc., Lawrence, Aug. 1983.

Onstott, R. G., R. K. Moore, S. Gogineni, and C. V. Delker, Four years of low altitude sea ice broadband backscatter measurements, IEEE J. Oceanic Eng., OE-7(1), 44-50, 1982a.

Onstott, R. G., R. K. Moore, and S. Gogineni, Radar backscatter measurements from Arctic Sea ice under summer conditions, Proceedings of the Workshop on Sea Ice and Icebergs 1980, NASA Goddard Space Flight Center, Greenbelt, Md., April 1982b.

Onstott, R. G., R. K. Moore, and W. F. Weeks, Surface-based scatterometer results of Arctic Sea ice, IEEE Trans. Geosci. Electron., GE-17(3), 78-85, 1979.

Parashar, S. K., A. W. Biggs, A. K. Fung, and R. K. Moore, Investigation of radar discrimination of sea ice, Proceedings of 9th International Symposium on Remote Sensing of Environment, Univ. of Mich., Ann Arbor, 1974.

Peteherych, S., SEASAT scatterometer measurement, paper presented at URSI Commission F Symposium on Signature Problems in Microwave Remote Sensing of the Surface of the Earth, Lawrence, Kans., Jan. 5-8, 1981

Raney, R. K., RADARSAT--Canada's national radar satellite program, IEEE Geosci. and Remote Sensing Newsletter, 5-9, March 1982.

Rouse, J. W., Jr., Arctic ice type identification by radar, Proc. IEEE, 57, 605-614, 1969.

Ulaby, F. T., R. K. Moore, and A. K. Fung, Microwave Remote Sensing: Active and Passive, vol. 2, Radar Remote Sensing and Surface Scattering and Emission Theory, pp. 922-991, Addison-Wesley , Reading Mass., 1982.

Weeks, W. F., Sea-ice: The potential of remote sensing, Oceanus, 4(3), 39-47, Fall 1981.

Weeks, W. F., and N. Untersteiner, Sea-ice: NASA oceanic processes program status report, NASA Tech. Memo. 80233, July 1980.

S. P. Gogineni and R. G. Onstott, Remote Sensing Laboratory, University of Kansas, Center for Research, Inc., 2291 Irving Hill Drive—Campus West, Lawrence, KS 66045-2969.

(Received April 13, 1984; accepted June 7, 1984)